



Lower bounds to eigenvalues of the Schrödinger equation by solution of a 90-y challenge

Rocco Martinazzo^{a,b,1,2} and Eli Pollak^{c,1,2}

^aDipartimento di Chimica, Università degli Studi di Milano, 20133 Milano, Italy; ^bInstitute of Molecular Science and Technologies, Consiglio Nazionale delle Ricerche, 20133 Milano, Italy; and ^cChemical and Biological Physics Department, Weizmann Institute of Science, 76100 Rehovoth, Israel

Edited by Gustavo E. Scuseria, Rice University, Houston, TX, and accepted by Editorial Board Member Peter J. Rossky May 20, 2020 (received for review April 19, 2020)

The Ritz upper bound to eigenvalues of Hermitian operators is essential for many applications in science. It is a staple of quantum chemistry and physics computations. The lower bound devised by Temple in 1928 [G. Temple, *Proc. R. Soc. A Math. Phys. Eng. Sci.* 119, 276–293 (1928)] is not, since it converges too slowly. The need for a good lower-bound theorem and algorithm cannot be overstated, since an upper bound alone is not sufficient for determining differences between eigenvalues such as tunneling splittings and spectral features. In this paper, after 90 y, we derive a generalization and improvement of Temple's lower bound. Numerical examples based on implementation of the Lanczos tridiagonalization are provided for nontrivial lattice model Hamiltonians, exemplifying convergence over a range of 13 orders of magnitude. This lower bound is typically at least one order of magnitude better than Temple's result. Its rate of convergence is comparable to that of the Ritz upper bound. It is not limited to ground states. These results complement Ritz's upper bound and may turn the computation of lower bounds into a staple of eigenvalue and spectral problems in physics and chemistry.

energy eigenstates | lower bound | quantum chemistry | lattice models

The Ritz upper bound to eigenvalues (1) of operators is an essential part of any advanced quantum mechanics course (2) for obvious reasons. It is fundamental for computation of energy eigenstates and used extensively in physics and chemistry. Deriving a lower-bound theorem which would converge to the numerically exact eigenvalue at the same rate as the Ritz upper bound is a challenge that has remained open but is of interest to practically anyone computing eigenvalues and for many reasons. It would provide a rigorous estimate to the accuracy of the approximate upper-bound computation. Without knowledge of a lower bound it is impossible to bound eigenvalue differences, needed for spectra and tunneling splittings.

Temple (3) presented a lower-bound theorem for the eigenvalues in 1928; however, its rate of convergence is highly unsatisfactory; in some cases it is orders of magnitude slower than the Ritz upper-bound convergence rate (4). The theorem has been applied to higher eigenvalues, but the result for any eigenstate depends on having a “good” lower bound for the neighboring higher-energy state (5); however, the precise nature of this lower bound is unknown except for the ground state. Many authors have attempted to improve upon Temple's result, to no avail; a representative list may be found in refs. 5–12. In the past year a different approach has been suggested and shown to improve upon Temple's method (13, 14). It improved upon Temple's original bound; however, to ensure rapid convergence it was necessary to use an approximate estimate for overlap matrix elements (14).

In this article, we present a rigorous lower-bound expression. It generalizes Temple's formula and is not limited to the ground-state eigenvalue. The input needed for its application is similar to the input used for determining the parallel Ritz upper bound to the eigenvalue. This implies that it becomes possible to obtain simultaneously both an upper

and a lower bound to the eigenvalue under consideration employing the Ritz eigenstates, although the lower-bound method becomes more involved as one goes to higher-lying states. The method of derivation also sheds light on some aspects of Temple's formula and especially its use for excited states (7).

Application of the method makes use of the Lanczos algorithm (15) of constructing an orthonormal basis of the Krylov subspace (16) obtained by repeated operation of the Hamiltonian operator (denoted as H) on an initial trial state. To exemplify the practical usefulness of the lower bound we apply it to the ground state of some nontrivial Heisenberg (17) and Hubbard (18) lattice models. Implementation of the method to excited states is presented in *SI Appendix*. We find that the convergence rate and the accuracy of the lower bound are competitive with those of Ritz's variational upper bound.

Lower-Bound Theory

Background. We refer all along to a Hamiltonian operator, but from the outset it should be clear that the theory presented is valid for any Hermitian operator with a discrete spectrum. The exact eigenvalues (in increasing order) and (normalized) eigenstates of the Hamiltonian are denoted respectively as $\varepsilon_j, |\varphi_j\rangle, j = 0, 1, \dots$. We choose an orthonormal basis set $\{|\Psi_j\rangle\}_{j \in \mathbb{N}}$ and construct a finite $L + 1$ -dimensional

Significance

In quantum theory a celebrated theorem due to Ritz provides upper bounds to eigenvalues of Hermitian operators. An upper bound alone, though, is not sufficient for determining the error of the computed eigenvalues, and cannot be used to assess the quality of energy differences, such as those needed for predicting the position of spectral lines or the energetics of a chemical reaction. The search for a complementary “lower-bound theorem” started in the early days of quantum mechanics but little progress has been reported since a seminal 1928 result of Temple whose accuracy was far less than that of the upper bound. Here, we settle this issue by devising rigorous lower bounds whose accuracy is similar to that of the upper bounds.

Author contributions: R.M. and E.P. wrote the paper; E.P. planned research; and R.M. performed the numerical calculations.

The authors declare no competing interest.

This article is a PNAS Direct Submission. G.E.S. is a guest editor invited by the Editorial Board.

Published under the PNAS license.

Data deposition: A Fortran code to compute the lower-bound estimates described in this paper is freely available on GitHub: <https://github.com/rocco-martinazzo/LowerBounds>.

¹To whom correspondence may be addressed. Email: rocco.martinazzo@unimi.it or eli.pollak@weizmann.ac.il.

²R.M. and E.P. contributed equally to this work.

This article contains supporting information online at <https://www.pnas.org/lookup/suppl/doi:10.1073/pnas.2007093117/-DCSupplemental>.

First published June 29, 2020.

representation of the Hamiltonian with the help of the projector P_L onto the space spanned by the first $L + 1$ basis states,

$$P_L = \sum_{j=0}^L |\Psi_j\rangle \langle \Psi_j| \quad H_L = P_L H P_L. \quad [1]$$

This finite-dimensional Hamiltonian is diagonalized. $|\Phi_j^{(L)}\rangle$ and $\lambda_j^{(L)}$ denote its eigenvectors and eigenvalues, respectively, with $j = 0, 1, \dots, L$. Ritz's variational principle (19) assures us that for any $L \geq 0$ the resulting eigenvalues are upper bounds to the exact ones; that is, $\lambda_j^{(L)} \geq \varepsilon_j$.

The Hamiltonian operator may be either analytic or represented as a huge $N \times N$ matrix that cannot be numerically diagonalized by standard similarity transformations and/or factorizations which demand $\mathcal{O}(N^3)$ operations. However, matrix-vector multiplications may yet be feasible ($\mathcal{O}(N^2)$). The dimensionality $L + 1$ of the chosen orthonormal basis set would be typically much smaller than N , so that diagonalization in this space is fast and creates no difficulties.

Introducing $\mathcal{P}_k = |\varphi_k\rangle \langle \varphi_k|$, the projector onto the $(k + 1)$ th exact eigenstate, any of the Ritz upper bounds may also be expressed as

$$\lambda_k^{(L)} = a_k \varepsilon_k + (1 - a_k) \bar{\lambda}_k^{(L)}, \quad [2]$$

where $a_k = \langle \Phi_k^{(L)} | \mathcal{P}_k | \Phi_k^{(L)} \rangle = |\langle \Phi_k^{(L)} | \varphi_k \rangle|^2$ and what we term as the residual energy $\bar{\lambda}_k^{(L)}$ is defined as

$$\bar{\lambda}_k^{(L)} = \frac{\langle \Phi_k^{(L)} | H - \varepsilon_k \mathcal{P}_k | \Phi_k^{(L)} \rangle}{1 - a_k}. \quad [3]$$

For notational convenience, we have omitted the L dependence of the coefficients a_k . These coefficients are of course unknown. The identity in Eq. 2 allows us to replace them with the unknown residual energy since

$$\frac{1 - a_k}{a_k} = \frac{\lambda_k^{(L)} - \varepsilon_k}{\bar{\lambda}_k^{(L)} - \lambda_k^{(L)}}. \quad [4]$$

The advantage of using the residual energy is that we know more about it than about the coefficients. Due to the ordering of the eigenvalues one may readily derive bounds to it. For example, for the ground state, the Ritz theorem assures us that $\bar{\lambda}_0^{(L)} \geq \max\{\varepsilon_1, \lambda_0^{(L)}\}$. More on this may be found in *SI Appendix*.

As shown below, Eq. 4, despite its simplicity, proves to be a key identity that allows one to do away with approximate overlaps, such as those used for instance in equation 2.22 of ref. 14. As a result, the present lower bound is rigorous and the resulting expression (Eq. 13 below) is more compact and simpler to implement.

Temple's Bound Revisited. We are interested in deriving a lower-bound expression to the eigenvalue ε_k . Using the corresponding approximate eigenvector to the $k + 1$ th state obtained by diagonalizing the projected Hamiltonian H_L ($L \geq k$), we may construct a normalized state $|\Phi_{\perp,k}^{(L)}\rangle$ which lies in the orthogonal complement of the P_L -projected space,

$$|\Phi_{\perp,k}^{(L)}\rangle = \frac{1}{\sigma_{L,k}} \left(\lambda_k^{(L)} - H \right) |\Phi_k^{(L)}\rangle. \quad [5]$$

Here,

$$\sigma_{L,k}^2 = \langle \Phi_k^{(L)} | (\lambda_k^{(L)} - H)^2 | \Phi_k^{(L)} \rangle \quad [6]$$

denotes the energy variance associated with $|\Phi_k^{(L)}\rangle$. The construction ensures that $P_L |\Phi_{\perp,k}^{(L)}\rangle = 0$, that is, that $|\Phi_{\perp,k}^{(L)}\rangle$ lies in the

complementary space, since $|\Phi_k^{(L)}\rangle$ is the $(k + 1)$ th eigenvector of H_L .

Taking the scalar product of Eq. 5 with the exact eigenstate of the Hamiltonian $|\varphi_k\rangle$, squaring and rearranging gives a central identity and inequality

$$\begin{aligned} \left(\lambda_k^{(L)} - \varepsilon_k \right)^2 &= \sigma_{L,k}^2 \frac{|\langle \varphi_k | \Phi_{\perp,k}^{(L)} \rangle|^2}{a_k} \\ &\leq \sigma_{L,k}^2 \left[\frac{1 - a_k}{a_k} - \frac{1}{a_k} \sum_{j=0, \dots, L}^{j \neq k} |\langle \varphi_k | \Phi_j^{(L)} \rangle|^2 \right]. \quad [7] \end{aligned}$$

The last line follows from completeness, $P_L + |\Phi_{\perp,k}^{(L)}\rangle \langle \Phi_{\perp,k}^{(L)}| \leq I$.

Eq. 7 is already instructive. The inequality sign in the second line remains if one ignores the second term in the square brackets (the overlap ratios). Using Eq. 4, remembering the upper-bound property $\lambda_k^{(L)} \geq \varepsilon_k$ and rearranging, one obtains Temple's lower-bound expression

$$\varepsilon_k \geq \lambda_k^{(L)} - \frac{\sigma_{L,k}^2}{\bar{\lambda}_k^{(L)} - \lambda_k^{(L)}}, \quad [8]$$

where the remaining unknown quantity is the residual energy $\bar{\lambda}_k^{(L)}$. For the ground state, we already noted that $\bar{\lambda}_0^{(L)} \geq \varepsilon_1$ so that a suitable lower bound to the first excited state would give a calculable lower bound. As is discussed below, obtaining good estimates to the residual energy leads to significant improvement in the quality of the lower-bound estimate.

Improved Temple's Bound. An essential improvement of Temple's lower bound comes from deriving practical expressions for the overlap ratios appearing in the second line of Eq. 7. Introducing the projector onto the complementary space $Q_L = 1 - P_L$ we note that

$$\langle \varphi_k | H | \Phi_j^{(L)} \rangle = \varepsilon_k \langle \varphi_k | \Phi_j^{(L)} \rangle = \langle \varphi_k | H_L + Q_L H P_L | \Phi_j^{(L)} \rangle. \quad [9]$$

Using Eq. 5 to replace $Q_L H | \Phi_j^{(L)} \rangle$ with $-\sigma_{L,j} |\Phi_{\perp,j}^{(L)}\rangle$, noting that $H_L | \Phi_j^{(L)} \rangle = \lambda_j^{(L)} | \Phi_j^{(L)} \rangle$, and rearranging Eq. 9 we find, upon squaring,

$$\left(\lambda_j^{(L)} - \varepsilon_k \right)^2 = \frac{\sigma_{L,j}^2 |\langle \varphi_k | \Phi_{\perp,j}^{(L)} \rangle|^2}{|\langle \varphi_k | \Phi_j^{(L)} \rangle|^2}. \quad [10]$$

In turn, this leads to the result

$$\frac{|\langle \varphi_k | \Phi_j^{(L)} \rangle|^2}{a_k} = \frac{\left(\lambda_k^{(L)} - \varepsilon_k \right)^2}{\left(\lambda_j^{(L)} - \varepsilon_k \right)^2} \frac{\sigma_{L,j}^2}{\sigma_{L,k}^2} R_{jk}^{(L)}, \quad [11]$$

$$R_{jk}^{(L)} \equiv \frac{|\langle \varphi_k | \Phi_{\perp,j}^{(L)} \rangle|^2}{|\langle \varphi_k | \Phi_{\perp,k}^{(L)} \rangle|^2} \geq 0. \quad [12]$$

Inserting Eq. 11 into the inequality of Eq. 7 and using Eq. 4 give the illuminating expression

$$\varepsilon_k \geq \lambda_k^{(L)} - \frac{\sigma_{L,k}^2}{\bar{\lambda}_k^{(L)} - \lambda_k^{(L)}} \left[1 + \sum_{j=0, \dots, L}^{j \neq k} \frac{\sigma_{L,j}^2}{\left(\lambda_j^{(L)} - \varepsilon_k \right)^2} R_{jk}^{(L)} \right]^{-1}. \quad [13]$$

Since the term in brackets appearing in the denominator on the right-hand side (r.h.s.) is larger than unity, it is evident that Eq. 13 improves upon Temple's result (3) (Eq. 8).

To complete the improved lower-bound theory it is necessary to know the coefficients $R_{jk}^{(L)}$. If, as is the case when using the

Lanczos method (15), one creates a tridiagonal matrix representation of the Hamiltonian, then the only term in it that connects the P_L space with the Q_L space is of the form $H_{L+1,L}|\Psi_{L+1}\rangle\langle\Psi_L|$. Therefore, from the definition of the perpendicular state (Eq. 5) we find that $|\langle\varphi_k|\Phi_{\perp,j}^{(L)}\rangle|^2 = |\langle\varphi_k|Q_L H|\Phi_j^{(L)}\rangle|^2/\sigma_{L,j}^2 = |H_{L+1,L}|^2|\langle\varphi_k|\Psi_{L+1}\rangle|^2|\langle\Psi_L|\Phi_j^{(L)}\rangle|^2/\sigma_{L,j}^2$. Similarly, one also has that

$$\sigma_{L,j}^2 = |\langle\Phi_j^{(L)}|H Q_L H|\Phi_j^{(L)}\rangle|^2 = |H_{L+1,L}|^2|\langle\Psi_L|\Phi_j^{(L)}\rangle|^2 \quad [14]$$

so that one readily finds that all of the coefficients $R_{jk}^{(L)} = 1$. We note that Eq. 14 is also useful for the computation of the variances needed for implementation of the lower-bound expression (Eq. 13). The matrix element $H_{L+1,L}$ is known from the Lanczos construct and the overlap $|\langle\Psi_L|\Phi_j^{(L)}\rangle|^2$ is obtained when diagonalizing the (small) Lanczos tridiagonal matrix. Since the Lanczos construct is an important element in the lower-bound theory as presented, we provide a short review of the Lanczos method in *SI Appendix*.

More generally, a sufficient condition for the coefficients $R_{jk}^{(L)}$ to equal unity is that there is a single doorway state $|\Omega\rangle$ connecting the P_L and Q_L spaces in the Hamiltonian matrix (i.e., that $Q_L H|\Phi\rangle = f(\Phi)|\Omega\rangle$ holds for any $|\Phi\rangle$ in the P_L space, with $f(\Phi)$ a c number). In that case the variance of the j th eigenstate follows as $\sigma_j^2 = |\langle\Omega|H|\Phi_j\rangle|^2$, similarly to Eq. 14 (*SI Appendix*).

Practical Considerations. To implement the theory it is necessary to address two further issues: 1) To obtain a numerical value for the r.h.s. of Eq. 13 it seems to be necessary to know the eigenvalue (ε_k) that we want to bound. 2) One has to specify how to estimate the residual energy $\bar{\lambda}_k^{(L)}$ (defined in Eq. 3).

With regard to issue 1 we note that if one knows a lower bound to the eigenvalue, then one can use it (under reasonable circumstances, as discussed below) in the expression to obtain an improved lower bound. Then one iterates the result by inserting the new lower bound on the r.h.s until convergence. Specifically, consider first the ground state and a basis with a single state $L=0$. The sums disappear and one regains Temple's lower bound for the ground-state energy which we denote as $\varepsilon_{-,0}^{(0)}$. Here, the minus subscript implies a lower bound, the zero subscript is for the ground state, and the (0) superscript notes that the lower bound was obtained with only one basis state. Increasing the space to two states, it becomes possible to replace ε_0 on the r.h.s. of Eq. 13 with the known $\varepsilon_{-,0}^{(0)}$ since for any $j \geq 1, L \geq 1, \lambda_j^{(L)} - \varepsilon_0 \leq \lambda_j^{(L)} - \varepsilon_{-,0}^{(0)}$. This enables us to estimate $\varepsilon_{-,0}^{(1)}$ from Eq. 13. We may now reinsert $\varepsilon_{-,0}^{(1)}$ into the r.h.s. to further improve the lower bound and iterate until convergence. We then have for the ground state the lower-bound expression

$$\varepsilon_0 \geq \lambda_0^{(L)} - \frac{\sigma_{L,0}^2}{\bar{\lambda}_0^{(L)} - \lambda_0^{(L)}} \left[1 + \sum_{j=1}^L \frac{\sigma_{L,j}^2}{\left(\lambda_j^{(L)} - \varepsilon_{-,0}^{(L)}\right)^2} \right]^{-1} \quad [15]$$

This procedure may be implemented for any eigenvalue but one must be careful. The Ritz theorem ensures the inequality $0 \leq \lambda_j^{(L)} - \varepsilon_k \leq \lambda_j^{(L)} - \varepsilon_{-,k}^{(L-1)}$ for $j = k+1, \dots, L$. For $j \leq k-1$ there is no guarantee that $\varepsilon_k \geq \lambda_j^{(L)}$. But if the basis set is sufficiently large and the change of the approximate energy $\lambda_{k+1}^{(L)}$ of the $(k+1)$ th state with increasing dimensionality L is much less than the distance $\lambda_{k+1}^{(L)} - \lambda_k^{(L)}$, one may well assume that

$\varepsilon_k \geq \lambda_j^{(L)}, j = 0, \dots, k-1$. Then $0 \leq \varepsilon_k - \lambda_j^{(L)} \leq \lambda_k^{(L)} - \lambda_j^{(L)}$. We thus have the central lower-bound expression

$$\varepsilon_k \geq \lambda_k^{(L)} - \frac{\sigma_{L,k}^2}{\bar{\lambda}_k^{(L)} - \lambda_k^{(L)}} \left[1 + \sum_{j=0, \dots, L}^{j \neq k} \frac{\sigma_{L,j}^2}{\left(\lambda_j^{(L)} - \mu_{jk}^{(L)}\right)^2} \right]^{-1}, \quad [16]$$

where $\mu_{jk}^{(L)} = \lambda_k^{(L)}$ for $j < k$ and $\mu_{jk}^{(L)} = \varepsilon_{-,k}^{(L)}$ otherwise.

There remains issue 2, the resolution of the residual energy $\bar{\lambda}_k^{(L)}$. As usually implemented for Temple's lower bound (4), it suffices to obtain a lower bound for this residual energy. For the ground state we already noted that $\bar{\lambda}_0^{(L)} \geq \max\{\lambda_0, \varepsilon_1\}$ so that a straightforward procedure is to use Weinstein's lower bound (20) for the first excited-state energy; that is, $\varepsilon_1 \geq \lambda_1^{(L)} - \sigma_{L,1}$.

Even for the ground state, there remains a small point to be clarified. Weinstein's lower bound is valid when $\lambda_1^{(L)} \leq (\varepsilon_1 + \varepsilon_2)/2$ (20, 21). How does one objectively know that this condition is obeyed? It is trivial to see that $\bar{\lambda}_0^{(L)} \geq \lambda_0^{(L)}$ so one may set $\bar{\lambda}_0^{(L)}$ to be incrementally larger than $\lambda_0^{(L)}$. As one increases the size of the basis set it is to be expected that also the Ritz estimate for the first excited state $\lambda_1^{(L)}$ will become sufficiently accurate so that it would become possible to switch to the Weinstein lower bound. One may identify the point at which this happens by following the magnitude of the Weinstein lower bound at each increase of the basis set. At first, increasing the basis set will rapidly lower the first excited-state eigenvalue $\lambda_1^{(L)}$. When it becomes quite accurate, one expects that also the variance associated with it will become smaller so that the Weinstein lower bound will start increasing with increasing L . From this point onward one may assume with some certainty that the Weinstein lower bound is valid. As the computation proceeds with increasing dimensionality, one may further improve upon the Weinstein estimate by using the lower bound obtained for the first excited state (Eq. 16). However, it is not known in general that $\bar{\lambda}_k^{(L)} \geq \varepsilon_{k+1}$ so that for $k \geq 1$ one needs more sophistication for evaluating a lower bound for the residual energy. This is presented in *SI Appendix*.

Implementation to Lattice Models

To illustrate the proposed lower-bound method for the ground state as given in Eq. 15 we applied it to some nontrivial Heisenberg and Hubbard lattice models of reasonable size such that they may be converged numerically with the iterative Lanczos diagonalization approach (22, 23) (*Computational Methods and Models*). This convergence amounts to a full diagonalization of the problem, i.e., a full configuration-interaction calculation.

The procedure used to obtain a lower bound for the residual energy $\bar{\lambda}_0^{(L)}$ is shown in Fig. 1. Fig. 1, *Left* and Fig. 1, *Right* correspond, respectively, to an antiferromagnetic Heisenberg model with exchange coupling J and a Hubbard model with hopping energy t and on-site Coulomb repulsion $U = 4t$. These two models are sketched in Fig. 2. The open circles in Fig. 1 show the Ritz eigenvalues as functions of the dimensionality of the basis set for the lowest few states. The dashed lines in Fig. 1 show the Weinstein lower bounds for the ground and first excited states. One notes how initially these lower bounds drop rapidly with increasing L and then start increasing. In both cases the recursion was started from a random initial vector, a rather poor approximation to the ground state. Several tens of iterations are needed before even the Ritz upper bounds become meaningful. The resulting lower bounds used for the residual energy $\bar{\lambda}_0^{(L)}$ are shown as the red symbols in Fig. 1. As discussed above, initially the estimate is taken to be incrementally larger than the ground-state energy; then after finding a minimum in the

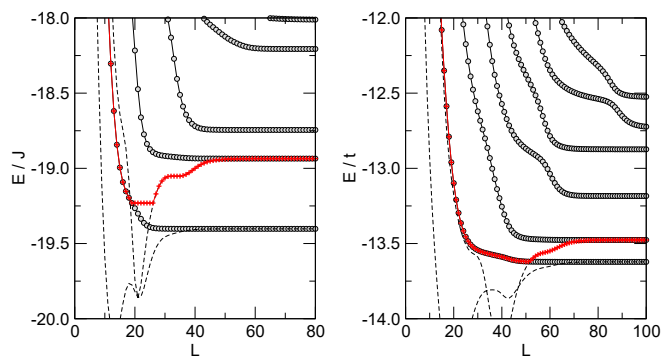


Fig. 1. The procedure used to estimate the residual energy. Open circles connected by solid lines show the lowest Lanczos eigenvalues as functions of the dimensionality L . The dashed lines are the Weinstein lower bounds to the ground-state and first excited-state energies. The red symbols show our choice of the lower bound to the residual energy $\bar{\lambda}_0$. *Left* and *Right* panels, respectively, show the results for the Heisenberg and Hubbard models depicted in Fig. 2. Energies are in units of the exchange coupling J (*Left*) and in units of the hopping integral t (*Right*).

Weinstein lower bound as a function of L we switch to the Weinstein lower bound.

The accuracy of the lower bound to the ground-state energy is compared with the accuracy of the Ritz upper bound in Fig. 3. The distance from the converged energy is plotted on a logarithmic scale as a function of the dimensionality of the Lanczos basis set, for both the upper and the lower bound. In Fig. 3, *Top Left* and *Top Right* correspond to the same two models considered in Fig. 1. Both *Top Left* and *Top Right* show that the convergence rates of the lower and upper bounds are essentially the same: As soon as Weinstein's lower bound for the first excited state becomes a reliable lower bound to the residual energy $\bar{\lambda}_0^{(L)}$ (this occurs at $L \sim 30$ and 50 , for Fig. 3, *Top Left* and *Top Right*, respectively), the ground-state lower bound provided by Eq. 15 becomes comparable in accuracy to the Ritz upper bound. The lower bounds for the Heisenberg square lattice (Fig. 3, *Top Left*) are somewhat more accurate than for the Hubbard square lattice (Fig. 3, *Top Right*) which gives the worst lower bounds out of all of the various models we considered, most likely because of the small energy gap involved (Fig. 1). Further results are presented in *SI Appendix*, Figs. S2–S5, showing accuracy similar or superior to that shown in Fig. 3, *Left* column.

Can one further improve the lower-bound estimate? As shown in Fig. 3, *Bottom Left* and *Bottom Right*, when using the numerically exact value of the residual energy, the lower-bound error becomes smaller than the upper-bound error. Of course, knowing the exact residual energy is the same as knowing the exact eigenvalue. This is of little practical use; however, the comparison shows that any further improvement in estimation of the residual energy will lead to even better improvement of

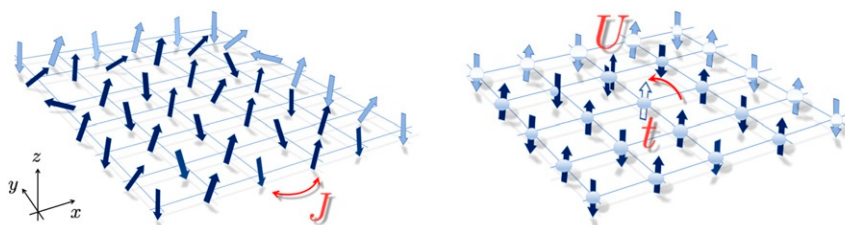


Fig. 2. Schematics illustrating the models considered in the main text. (*Left*) We show the 5×6 unit cell of the antiferromagnetic Heisenberg square lattice model with exchange coupling J . (*Right*) We sketch the 4×4 unit cell of the Hubbard square lattice model at half-filling. In this case t is the hopping energy and U the Coulomb repulsion. Shaded objects represent periodic images.

the lower-bound estimate. Stated differently, the fundamental inequality of Eq. 7, on which our lower-bound theory relies, is tighter than the truncation error accompanying the Ritz estimate, and the quality of the proposed lower bounds can in principle exceed that of the upper ones.

The results presented in Fig. 3 are on a logarithmic scale, showing that the convergence rate of the upper and lower bounds is similar. In Fig. 4, *Left* we plot the ratio of the lower- to upper-bound errors as a function of the logarithm of the error of the upper bound. One notes that over a region of 10 decades the ratio stays quite constant and in most cases is less than 5, attesting to the quality of the lower bound. Fig. 4, *Right* shows the ratio of the difference between Temple's lower bound (based on $|\Phi_0^{(L)}\rangle$) and using the same lower bound for the residual energy $\bar{\lambda}_0^{(L)}$ and the improved lower bound of Eq. 15 to the error in the upper bound. This ratio is also plotted as a function of the error in the upper-bound Ritz estimate. The gain in accuracy coming from the implementation of Eq. 15 is considerable, especially in light of the minor additional effort required to evaluate it. This comparison clearly demonstrates the improvement due to the present generalization of Temple's lower bound.

Inspection of the results shows that the quality of the lower bound depends on the system studied. Two factors control the quality of the lower bound. One is the magnitude of the variances. The more important one is the estimate of the residual energy. In all of the computations we used the Weinstein lower bound for the first excited-state energy and the property that the residual energy is larger than the first excited-state energy. In reality the residual energy may be much larger than the first excited-state energy, as is the case for the Hubbard square lattice model studied here.

In the cases presented in this paper, the error ratio of the lower bound to the Ritz upper bound is typically less than a factor of 5, and in the worst case it is a factor of 20. The improvement over Temple's lower bound is typically an order of magnitude or more. These results were also obtained for a variety of lattice models as reported in *SI Appendix*. They may thus be considered as characteristic for these models. The central difficulty is in the estimate of the residual energy $\bar{\lambda}_0^{(L)}$. As shown in Fig. 3 when one uses the numerically exact values, the lower-bound error becomes smaller than the upper-bound error. Further improvements in the estimate of the residual energy are possible, especially when obtaining also estimates on the upper and lower bounds for the first few excited states as discussed in *SI Appendix*.

Summary and Conclusions

We have presented a rigorous systematic improvement over the 90-y-old Temple lower bound. The improved lower bound is tight, converging as fast as the upper bound for a variety of lattice models, even though the numerics are initiated with a random vector. The applications here were limited to models which may still be converged numerically to the exact answer to show the efficacy of the method, but just as the Ritz result is useful as an

upper bound even when strict diagonalization is no longer possible, so is the case for the lower-bound expression presented here. The lower-bound estimates may also be used to speed up inverse iteration methods for computing accurate eigenvectors and thus physical properties (through, e.g., the one- and two-body Green's functions). The information needed is essentially the same as for the upper bounds so that one may obtain simultaneously upper and lower bounds. The gain is a quantitative estimate of the accuracy of a given computation, which is of paramount importance when convergence is out of reach.

The uses of the method go beyond lattice models; for example, one may obtain estimates on rovibrational energy levels of molecules (24) and tunneling splittings. Having good upper and lower bounds for a given eigenvalue enables one to obtain also upper and lower bounds on level differences, which are important when considering spectra, tunneling splittings, energy barriers, or reaction energies.

There is reason to believe that the method would be useful also for energies of real atoms and molecules. In principle the Coulomb potential usually cause matrix elements such as $\langle \Psi | \hat{H}^n | \Psi \rangle$ to diverge for $n \geq 3$, invalidating the straightforward application of the Lanczos method. However, in most applications, one uses a simple one-electron basis set (typically, an atom-centered set of Gaussians) to create the Hamiltonian matrix, thereby smoothing the Coulomb cusps and turning the problem into a basis-set convergence issue (25). This is analogous to the situation with Hubbard models as studied in this paper. Diagonalization of such a large matrix becomes prohibitive when increasing the size of the system, but a limited number of matrix-vector multiplications are still possible. In contrast to other $\mathcal{O}(N^2)$ methods such as the Jacobi–Davidson algorithm (26, 27),

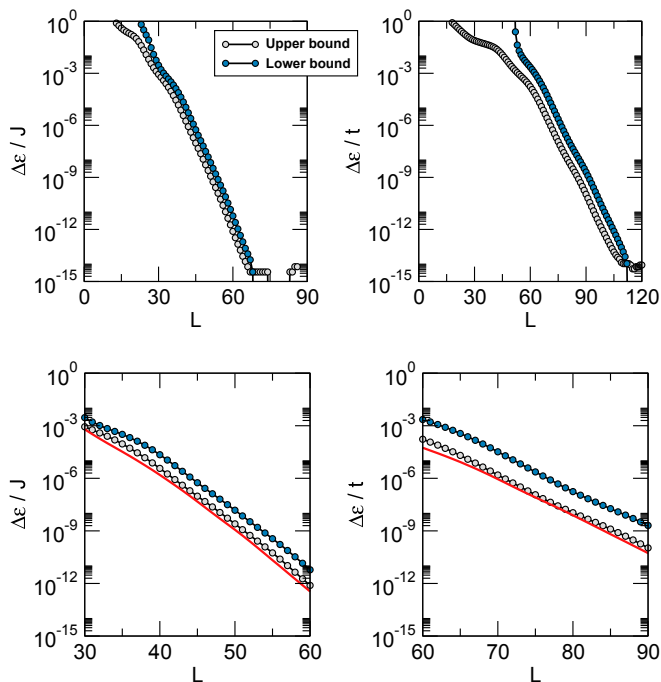


Fig. 3. Comparison of the ratio of the error of the lower bound to that of the upper bound as a function of the dimensionality L of the Lanczos iteration. *Top Left* corresponds to the 5×6 Heisenberg model and *Top Right* to the 4×4 Hubbard model. Gray and blue symbols show the upper- and lower-bound errors, respectively. *Bottom Left* and *Bottom Right* provide a close-up of *Top Left* and *Top Right*, showing also as the red lines the error in the lower-bound estimate when using the numerically exact value of the residual energy $\lambda_0^{(L)}$.

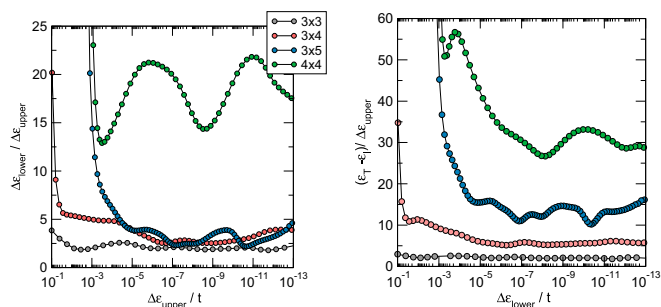


Fig. 4. (Left) The lower- to upper-bound error ratio for different $n \times m$ Hubbard models at half-filling, as indicated, with $U = 4t$ as a function of the error of the Ritz estimate. (Right) The ratio of the difference between Temple's (ϵ_T) lower bound and the improved (ϵ_I) lower bound of Eq. 15 to the error in the upper bound is plotted as a function of the Ritz estimate.

here, the upper and lower bounds tell us when the accuracy is sufficient, thus enabling a reduction in the number of matrix-vector multiplications that need to be performed.

In this paper we have limited ourselves to the computation of the ground-state energy, using the Weinstein lower bound to the first excited-state energy as a lower-bound estimate of the residual energy. This may be significantly improved if one also computes lower bounds to the higher-lying states using the present methodology instead of the Weinstein lower bound and then modifying the residual energy estimate. Computational examples for higher-lying states will be presented in future work.

In summary, the theory and results presented in this paper indicate that in the future, lower bounds may be as important as upper bounds when computing eigenvalues of Hermitian operators.

Computational Methods and Models

Lanczos calculations were performed with the $\mathcal{H}\Phi$ program package (22) which is based on the Lanczos-type eigenvalue solution. It is applicable to a broad range of quantum lattice models, i.e., arbitrary quantum lattice models with two-body interactions, including the Heisenberg, the Kitaev (28), the Hubbard, and the Kondo (29) lattice models. We considered here two kinds of model problems which find widespread applications in physics and chemistry. The first one is that of a set of spin-1/2 particles on a lattice, as described by the Heisenberg Hamiltonian

$$H_{\text{Heisenberg}} = J \sum_{\langle i,j \rangle} \mathbf{s}_i \mathbf{s}_j,$$

where \mathbf{s}_i is the spin-1/2 operator on the lattice site i , $\langle i, j \rangle$ stands for nearest-neighbor pairs only, and J is the coupling (or “exchange”) constant weighting the “exchange term” $\mathbf{s}_i \mathbf{s}_j$. This is the so-called Heisenberg XXX model (i.e., with isotropic interactions) and $J > 0$ ($J < 0$) for an antiferromagnetic (ferromagnetic) system. Its ground state is trivial for $J < 0$, for which a simple calculation shows that the parallel spin configuration is an eigenstate of the Hamiltonian and it has the smallest possible energy. It is less trivial for $J > 0$, which is the case considered in this work, since the “classical” antiferromagnetically ordered configuration is destroyed by the quantum fluctuations*, as a consequence, the spins tend to entangle in pairs and the “bonding pattern” fluctuates through the lattice. The lattice plays a distinctive role in this context, since it may introduce geometrical

*These are suppressed in the ferromagnetic case since the cross terms $s_i^+ s_j^-$ annihilate the ground state.

frustration in the system as happens, for instance, in the case of “triangular” lattices.

The second problem is the so-called Hubbard model described by the (second-quantization) Hamiltonian

$$H_{\text{Hubbard}} = \epsilon \sum_{i,\sigma} c_{i,\sigma} c_{i,\sigma}^\dagger - t \sum_{\langle i,j \rangle} c_{i,\sigma} c_{j,\sigma}^\dagger + U n_{i,\uparrow} n_{i,\downarrow},$$

where i identifies the (equivalent) lattice sites, $c_{i,\sigma}^\dagger$ ($c_{i,\sigma}$) creates (destroys) an electron in site i with spin $\sigma = \uparrow, \downarrow$, $n_{i,\sigma} = c_{i,\sigma}^\dagger c_{i,\sigma}$ is the number operator for the spin state σ on site i , ϵ is the “on-site” energy (conveniently set to zero in our case), t is the hopping energy between nearest neighbors, and $U > 0$ is the Coulomb repulsion experienced by two electrons placed in the same site. This is probably the most important and famous lattice model of interacting electrons (here in its simplest version with one orbital per site and a purely local interaction term) and the simplest one describing the fundamental competition between the kinetic (t) and the interaction (U) energy. When the latter prevails ($U \gg t$), if there is one electron per site (“half-filling”), the average site occupancy is one with

little fluctuations and neighboring electrons tend to have opposite spin; hence, the model reduces to the abovementioned antiferromagnetic Heisenberg model for a set of spin-1/2 particles (with $J \sim 4t^2/U$).

In our calculations, the lattice was always taken to be periodic and the simulation cell was limited to a finite number N of sites with periodic boundary conditions. The state-space \mathcal{H} has total dimension of 2^N for the Heisenberg problem and 4^N for the Hubbard one, but it is generally decomposed in smaller invariant subspaces upon exploiting the symmetry of the Hamiltonian (at least the SO(2) invariance which holds also in the presence of a magnetic field). In the models we used it has dimension 155,117,520 for the Heisenberg square lattice with a 5×6 unit cell and 165,636,900 for the Hubbard square lattice model at half-filling on a 4×4 unit cell.

Data Availability. A Fortran code to compute the lower-bound estimates described in this paper is freely available on GitHub: <https://github.com/rocco-martinazzo/LowerBounds>.

ACKNOWLEDGMENTS. This work was generously supported by a grant from the Yeda-Sela Foundation of the Weizmann Institute of Science.

1. W. Ritz, Über eine neue methode zur lösung gewisser variationsprobleme der mathematischen physik. *J. für die Reine Angewandte Math.* **1909**, 1–61 (1909).
2. C. Cohen-Tannoudji, F. Laloe, B. Diu, F. Laloe, *Quantum Mechanics* (Wiley, 1977).
3. G. Temple, The theory of Rayleigh's principle as applied to continuous systems. *Proc. R. Soc. A Math. Phys. Eng. Sci.* **119**, 276–293 (1928).
4. H. Nakashima, H. Nakatsuji, How accurately does the free complement wave function of a helium atom satisfy the Schrödinger equation?. *Phys. Rev. Lett.* **101**, 240406 (2008).
5. M. Cohen, T. Feldmann, A generalisation of Temple's lower bound to eigenvalues. *J. Phys. B Atom. Mol. Phys.* **12**, 2771–2779 (1979).
6. W. H. Miller, Improved equation for lower bounds to eigenvalues; bounds for the second-order perturbation energy. *J. Chem. Phys.* **50**, 2758–2762 (1969).
7. L. M. Delves, On the Temple lower bound for eigenvalues. *J. Phys. Math. Gen.* **5**, 1123–1130 (1972).
8. R. N. Hill, Tight lower bounds to eigenvalues of the Schrödinger equation. *J. Math. Phys.* **21**, 2182–2192 (1980).
9. A. Scrinzi, Lower bounds to the binding energies of $\text{td}\mu$. *Phys. Rev. A* **45**, 7787–7791 (1992).
10. M. G. Marmorino, P. Gupta, Surpassing the Temple lower bound. *J. Math. Chem.* **35**, 189–197 (2004).
11. M. G. Marmorino, A. Almayouf, T. Krause, D. Le, Optimization of the Temple lower bound. *J. Math. Chem.* **50**, 833–842 (2012).
12. T. Baumgratz, M. B. Plenio, Lower bounds for ground states of condensed matter systems. *New J. Phys.* **14**, 023027 (2012).
13. E. Pollak, An improved lower bound to the ground-state energy. *J. Chem. Theor. Comput.* **15**, 1498–1502 (2019).
14. E. Pollak, A tight lower bound to the ground-state energy. *J. Chem. Theor. Comput.* **15**, 4079–4087 (2019).
15. C. Lanczos, An iteration method for the solution of the eigenvalue problem of linear differential and integral operators. *J. Res. Natl. Bur. Stand.* **45**, 255 (1950).
16. A. N. Krylov, On the numerical solution of equation by which are determined in technical problems the frequencies of small vibrations of material systems. *News Acad. Sci. USSR* **7**, 491–539 (1931).
17. W. Heisenberg, Zur theorie des ferromagnetismus. *Z. Phys.* **49**, 619–636 (1928).
18. J. Hubbard, B. H. Flowers, Electron correlations in narrow energy bands. *Proc. R. Soc. Lond. Math. Phys. Sci.* **276**, 238–257 (1963).
19. J. K. L. MacDonald, Successive approximations by the Rayleigh-Ritz variation method. *Phys. Rev.* **43**, 830–833 (1933).
20. D. H. Weinstein, Modified Ritz method. *Proc. Natl. Acad. Sci. U.S.A.* **20**, 529–532 (1934).
21. A. F. Stevenson, On the lower bounds of Weinstein and Romberg in quantum mechanics. *Phys. Rev.* **53**, 199 (1938).
22. M. Kawamura et al., Quantum lattice model solver H Φ . *Comput. Phys. Commun.* **217**, 180–192 (2017).
23. R. Martinazzo, E. Pollak, 2020, LowerBounds. GitHub. <https://github.com/rocco-martinazzo/LowerBounds>. Deposited 20 April 2020.
24. H. G. Yu, Multi-layer Lanczos iteration approach to calculations of vibrational energies and dipole transition intensities for polyatomic molecules. *J. Chem. Phys.* **142**, 044106 (2015).
25. H. Nakatsuji, M. Ehara, Iterative CI general singles and doubles (ICIGSD) method for calculating the exact wave functions of the ground and excited states of molecules. *J. Chem. Phys.* **122**, 194108 (2005).
26. C. G. J. Jacobi, Über ein leichtes verfahren die in der theorie der säcularstörungen vorkommenden gleichungen numerisch aufzulösen. *J. Reine Angew. Math.* **1846**, 51–94 (1846).
27. E. R. Davidson, The iterative calculation of a few of the lowest eigenvalues and corresponding eigenvectors of large real-symmetric matrices. *J. Comput. Phys.* **17**, 87–94 (1975).
28. A. Kitaev, Anyons in an exactly solved model and beyond. *Ann. Phys.* **321**, 2–111 (2006).
29. S. Doniach, The Kondo lattice and weak antiferromagnetism. *Phys. B+C* **91**, 231–234 (1977).